Chemical Physics Letters 467 (2009) 424–429

Contents lists available at ScienceDirect

Chemical Physics Letters

journal homepage: www.elsevier.com/locate/cplett

Terahertz spectroscopy of L-proline in reverse aqueous micelles

Catherine C. Cooksey [1], Benjamin J. Greer [2], Edwin J. Heilweil *

Optical Technology Division, Physics Laboratory, National Institute of Standards and Technology (NIST), 100 Bureau Drive, Mailstop 8443, Building 216, Gaithersburg, MD 20899-8443, United States

ARTICLE INFO

Article history:
Received 11 September 2008
In final form 17 November 2008
Available online 21 November 2008

ABSTRACT

A new method for obtaining room-temperature terahertz (THz) absorption spectra of aqueous-phase biomolecules in the frequency range 1–21 THz (35 cm^{-1}–700 cm^{-1}) is reported. The spectrum for L-proline was acquired by solvating the amino acid within the nanometer-sized interior water pool of reverse micelles dispersed in transparent *n*-heptane. Terahertz spectra of H_2O, D_2O and the effect of L-proline concentration and micelle size are discussed, and the results are compared to spectra of solid-phase L-proline and Gaussian calculations.

Published by Elsevier B.V.

1. Introduction

Terahertz vibrational modes typically involve the low frequency, collective atomic motions of molecules, which include both inter- and intramolecular interactions. Thus, terahertz spectroscopy of biomolecules in aqueous environments is becoming an important approach for identifying their global and transient molecular structures as well as directly assessing hydrogen-bonding and other detailed environmental interactions [1–5]. However, a significant challenge in obtaining the terahertz absorption spectra of aqueous biomolecules is the high-molar absorptivity of room-temperature water in the spectral range of 0.5–10 THz (17 cm^{-1}–333 cm^{-1} with peak molar absorptivity of 9 L mol^{-1} cm^{-1} at 6 THz) [6].

In this Letter, we report a novel method for acquiring terahertz spectra of biomolecular species in liquid water at room temperature in nanoscale reverse micellar structures. To avoid bulk water absorption, we solvate biomolecules within the interior water pool of size-controlled reverse micelles dispersed in a transparent nonpolar solvent [7,8]. The highly soluble amino acid, L-proline (aqueous concentrations up to 6.7 mol L^{-1}), is encapsulated within aerosol-OT (AOT) reverse micelles dispersed in *n*-heptane, and is examined in the frequency range of 1–21 THz (33 cm^{-1}–700 cm^{-1}) by FTIR spectroscopy. The effect of L-proline concentration and reverse micelle size on the terahertz spectrum is reported, and the results are compared to the far-infrared spectra of solid-phase L-proline and Gaussian calculations of the zwitterionic structure (see Scheme 1). In addition, terahertz absorption spectra of H_2O and D_2O within reverse micelles formed from negatively charged and neutral surfactants (AOT and Brij-30, respectively) have also been carefully characterized for various reverse micelle sizes.

2. Experimental methods

Reverse micelle solutions were prepared from the following chemicals: sodium bis(2-ethylhexyl) sulfosuccinate (also known as aerosol-OT or AOT; Sigma–Aldrich), Brij-30 (Sigma–Aldrich), anhydrous *n*-heptane (Sigma–Aldrich), cyclohexane (Mallinkrodt), deionized water (~18 MΩ cm^{-1}), and perdeuterated water (Sigma–Aldrich) [9]. All chemicals were used as received. A stock solution of surfactant in nonpolar solvent was prepared and sonicated at 293 K for 40 min to ensure thorough mixing. Deionized water was added by micropipette (for example, 10–200 μL) to 10 ml aliquots of the stock solution to give the desired mole ratio, $w = [H_2O]/[\text{surfactant}]$. The resulting dispersion was sonicated for at least 20 min and then allowed to equilibrate overnight at room temperature. A successful sample preparation resulted in a clear, single-phase solution, as determined by visual inspection.

Specifically, all AOT reverse micellar dispersions had a total concentration of 0.024 mol L^{-1} AOT in *n*-heptane. The amount of water within the dispersion is reported by the mole ratio of water to surfactant: $w = [H_2O]/[\text{AOT}]$. The values of *w* for water-filled reverse micelles ranged from 1 to 20 for H_2O and 1 to 15 for D_2O. Brij-30 reverse micellar solutions had a concentration of 0.2 mol L^{-1} Brij-30 in cyclohexane and *w* values ranging from 1 to 5 for H_2O and D_2O. Within the range of values examined here ($w < 20$), *w* is found to vary linearly with the particle size for water-filled AOT and Brij-30 reverse micelles, and the hydrodynamic radii of these reverse micelles range from approximately 2 to 5 nm [10–12]. For the preparation of reverse micelles containing L-proline, a solution of L-proline (ICN Biomedicals, Inc.) [9] dissolved in water was added to the AOT stock solution with *w* values ranging from 1 to 12 for H_2O and $w = 5$ for D_2O. The mole fractions,

* Corresponding author. Fax: +1 1 0 301 975 6991.
E-mail address: edwin.heilweil@nist.gov (E.J. Heilweil).
[1] NIST/NRC Postdoctoral Fellow.
[2] NIST Summer Undergraduate Research Fellow, Carnegie Mellon University, Pittsburgh, PA 15213, United States.

0009-2614/$ - see front matter Published by Elsevier B.V.
doi:10.1016/j.cplett.2008.11.041

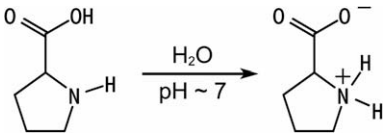

Scheme 1. Proline structure in water. Cooksey and Heilweil CPL.

χ_{Pro}, of L-proline in the aqueous solutions were 0.05, 0.11, and 0.20 (saturated, 6.7 mol L^{-1}).

Samples of solid L-proline were prepared from a 100 mg mixture of L-proline (mass fraction of L-proline is 0.1) and spectrophotometric grade, high-density polyethylene (Micro Powders, Inc. <10 μm particle size) [9]. Samples were pressed in a 13 mm diameter vacuum die at pressures of approximately 1.38 MPa (200 psi), resulting in a ~1.5 mm thick pellet.

All terahertz absorption measurements were made using a Nicolet Magna 550 Fourier transform infrared spectrometer (THz-FTIR), modified with a silicon-coated broadband beam-splitter and a deuterium triglyceral sulfide (DTGS) room-temperature detector fitted with a high-density polyethylene window. The sample compartment was purged for at least 45 min to eliminate water vapor before acquiring spectral scans. All spectra were taken at room temperature and represent an average of 192 interferometric scans with a spectral resolution of 4 cm^{-1}. Solution-phase samples were injected into a static cell equipped with two 3-mm thick high-resistivity (>2000 Ω cm) silicon windows obtained from ICL, Inc. [9]. The liquid pathlength was adjusted between 0.5 mm and 4.2 mm using Teflon spacers to maintain spectral intensities within the linear absorption range of the instrument (<2.5 optical density, OD).

Raw transmission spectra were converted into optical density units by ratioing sample spectra, T, against the reference spectra, T_0, according to the equation, $OD = -\log_{10}(T/T_0)$. Consistent with a previous absorption study of reverse micelles, we used the spectrum of the stock solution of the surfactant in the nonpolar solvent without the addition of water, $w = 0$, as the reference for a given micellar sample [13,14]. For the solid L-proline sample, a polyethylene-only pellet (total mass of 100 mg) served as the reference. Multiple ($\geqslant 3$) spectra were taken for each sample over several days to ensure consistency. Absorption measurements taken at various pathlengths enabled the calculation of the molar absorptivity spectrum of water in the reverse micelles according to Beer–Lambert Law. The relative error in molar absorptivity values derived from estimates of the error in concentrations and measured OD was found to be less than 10% (method of uncertainty analysis: type b, $k = 1$).

3. Results and discussion

3.1. Characterization of terahertz spectra for H_2O and D_2O in reverse micelles

Fig. 1 presents the molar absorptivity of water within reverse micelles of various w values. This spectral region has not previously been examined, despite publications of other far-infrared and infrared absorption spectra of water within reverse micelles [13–20]. The broad, librational absorption band, centered at 680 cm^{-1} in bulk H_2O and at 497 cm^{-1} in bulk D_2O, has been assigned to the restricted rotational motions of individual water molecules, while the 200 cm^{-1} absorption band in bulk H_2O and D_2O has been assigned to the intermolecular hydrogen-bond stretching mode [21]. Results concerning the librational absorption band will be discussed first, followed by a discussion of the hydrogen-bond stretching mode.

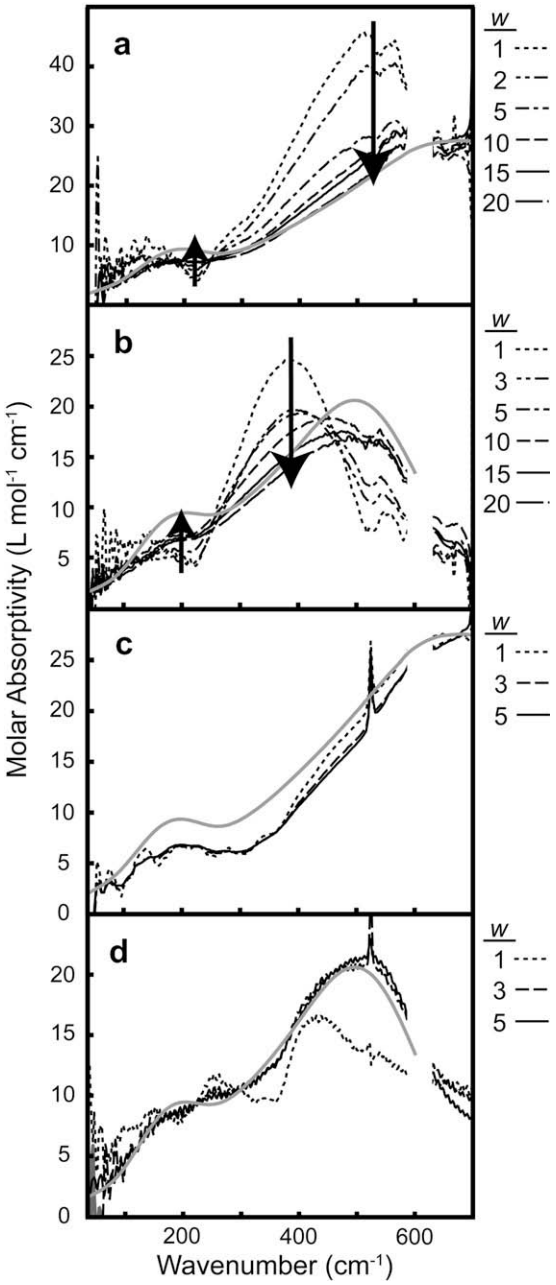

Fig. 1. Terahertz absorption spectra of water in reverse micelles of various w values compared to spectra of bulk H_2O [6] and D_2O [27] (solid gray curves), respectively. (a) H_2O in 0.024 mol L^{-1} AOT/heptane reverse micelles. (b) D_2O in 0.024 mol L^{-1} AOT/heptane reverse micelles. The arrows indicate the direction of spectral change as w increases. (c) H_2O in 0.2 mol L^{-1} Brij-30/cyclohexane reverse micelles. (d) D_2O in Brij-30/cyclohexane reverse micelles. The silicon windows of the static cell and polyethylene window of the detector result in negligible transmission between 585 cm^{-1} and 630 cm^{-1} preventing analyses in this region.

In Fig. 1a, the absorption spectrum of H_2O in AOT reverse micelles is compared to the bulk H_2O spectrum. Encapsulation of H_2O within AOT reverse micelles results in a red shift and increase in the maximum molar absorptivity of the librational band relative to the bulk H_2O spectrum. The magnitude of these changes increases as w decreases. The greatest red shift (160 cm^{-1}) and increase in molar absorptivity (17 L mol^{-1} cm^{-1}) occurs for the reverse micelles with $w = 1.1$. These spectral changes are consistent with previous measurements made by Schmuttenmaer and co-workers [13]. They reported the infrared spectra for H_2O in

AOT reverse micelles in the spectral region of 400 cm^{-1}–900 cm^{-1}. Their results indicate that the spectrum of water for AOT reverse micelles approaches the bulk water spectrum as w increases, essentially reproducing it for the largest reverse micelle investigated, $w = 40$ ($\sim 10^4$ water molecules per micelle). Schmuttenmaer and co-workers observed an isosbestic point near 620 cm^{-1}, which was interpreted as evidence for a two-state system. They successfully modeled the change in the librational band as a function of w assuming that water within the reverse micelles consists of two types: a combination of trapped and bound water molecules at the interface and bulk-like water residing within the interior of the water pool [13,22]. Schmuttenmaer and co-workers suggested that the red shift of the librational band of water in reverse micelles arises from weakening of the hydrogen-bonding network in the trapped and bound water region due to significant interfacial interaction and high degree of orientation relative to the surfactant headgroups. The enhancement in molar absorptivity was explained as either increased amplitude librations due to weakening of the hydrogen-bonding network or an increase in correlated molecular motion. Other groups have also successfully applied the two-state model to the OH (of H_2O) and OD (of HOD) high-frequency (2000 cm^{-1}–3600 cm^{-1}) stretching band of water in AOT reverse micelles [17–19]. Unfortunately, we cannot confirm the existence of an isosbestic point in this spectral region due to the strong absorption interference of polyethylene and the cell windows.

To extend our understanding of the water librational band in reverse micelles, we obtained terahertz spectra of the librational band of D_2O in AOT reverse micelles (Fig. 1b). The dependence of the peak position of the D_2O librational band on w is qualitatively similar to the case of H_2O within AOT reverse micelles, except that the band center is red-shifted due to the isotopic mass change. The librational band of D_2O in AOT reverse micelles occurs at lower frequencies than the bulk D_2O band, and the band red-shifts as the amount of water in the reverse micelle decreases. The greatest red shift (110 cm^{-1}) from the bulk D_2O librational band occurs for $w = 1.1$ reverse micelles. The maximum enhancement in molar absorptivity (4.4 L mol^{-1} cm^{-1}) for D_2O in AOT reverse micelles, relative to the bulk spectrum, occurs for $w = 1.1$. In contrast to H_2O in AOT reverse micelles, the molar absorptivity of D_2O for reverse micelles with $w > 1.1$ is less than bulk by as much as 4 L mol^{-1} cm^{-1}. In addition, a well-defined isosbestic point was not observed for the librational band of D_2O in AOT reverse micelles. Both of these observations indicate that the two-state model, as applied to H_2O in AOT reverse micelles, does not adequately describe D_2O in AOT reverse micelles.

To better understand the applicability of the core-shell model, we obtained terahertz absorption spectra of the water librational band in reverse micelles assembled from a surfactant with a neutral headgroup. Fig. 1c and d depict the molar absorptivity of H_2O and D_2O in Brij-30 reverse micelles. We find that the water librational band in Brij-30 reverse micelles is essentially equivalent to that of bulk water. The molar absorptivity and band position depend very little on w in comparison to H_2O and D_2O in AOT reverse micelles. The only exception to this is the water spectrum for D_2O in $w = 1.1$, Brij-30 reverse micelles. Each surfactant headgroup of Brij-30 includes a hydroxyl group, which is susceptible to deuteration upon exposure to D_2O. The effect of surfactant deuteration dominates the water spectrum for $w = 1.1$, Brij-30 reverse micelles because of the low water to surfactant mole ratio. Thus, the absorption spectra of water in Brij-30 reverse micelles do not support the hypothesis of distinct water types within the reverse micelle interior, as proposed by the core-shell model. The lack of distinct water types is reasonable because the hydrophilic headgroup of Brij-30 consists of a nonionic chain of four poly-oxo units terminated with a hydroxyl group, resulting in a less well-defined interfacial region in comparison to AOT, which has only a single charged headgroup to solvate. Thus, terahertz spectra indicate that the core-shell model is not generally applicable to water-filled reverse micelles, and that the librational absorption band is sensitive to interfacial interactions of water with the surfactant headgroup.

The entire lower frequency, intermolecular hydrogen-bond stretching band of water in reverse micelles has not been previously investigated in the far-infrared region at wavenumbers greater than 66 cm^{-1} [15]. Similar to the librational absorption band, the hydrogen-bond stretching band of H_2O and D_2O in AOT reverse micelles is red-shifted from that of bulk water, with the stretching band in the smallest micelles shifted by as much as 70 cm^{-1}. However, no clear enhancement in molar absorptivity is observed. Rather, the peak molar absorptivity of this band decreases by >2 L mol^{-1} cm^{-1} as the band shifts towards the band center of the bulk water. In contrast, the hydrogen-bond stretching mode of H_2O and D_2O does not red-shift in Brij-30 reverse micelles. The molar absorptivity of the H_2O mode in Brij-30 reverse micelles is 3 L mol^{-1} cm^{-1} less than for the corresponding mode in bulk water, and may be responsible for the decrease in molar absorptivity observed for the red edge of the librational band. The hydrogen-bond stretching band for D_2O in $w = 3$ and $w = 5$, Brij-30 reverse micelles is essentially equivalent to the bulk D_2O spectrum.

Previous studies of the OH- and OD-stretching mode of water in the mid-infrared report a blue shift upon encapsulation of water within reverse micelles [14,18,19]. The stretching band shifts to higher frequencies as w decreases, and has been traditionally interpreted as evidence for a weakened hydrogen-bonding network. The blue shift of this intramolecular mid-infrared band is consistent with red shift of the low frequency, intermolecular hydrogen-bond stretching band seen for water in AOT reverse micelles. However, we do not find any red-shifting of the hydrogen-bond stretching band for water in Brij-30 reverse micelles despite previous observations of blue-shifting of the OH and OD stretch for water within reverse micelles formed from other neutral surfactants [14,20].

3.2. Terahertz absorption spectra of aqueous L-proline in reverse micelles

Having measured and characterized the terahertz spectra of water within reverse micelles as a function of w, size, and surfactant, we investigated spectral changes for the addition of L-proline to the water phase. Fig. 2 shows absorption spectra of aqueous-phase L-proline within AOT reverse micelles where Fig. 2a and b contain difference spectra. To generate these spectra, we assumed that the contributions of L-proline and water are independent and additive. Thus, a spectrum of L-proline and water in reverse micelles with a given w was ratioed against the absorption spectrum of water in reverse micelles with the same w value to generate a difference spectrum of only L-proline in the reverse micelle. In Fig. 2a, all absorption spectra of L-proline within AOT reverse micelles have the same mole ratio of water to surfactant, $w = 1.1$; however, the mole fraction of L-proline, χ_{pro}, in water changes from 0.05 to 0.20. Three distinct absorption peaks (labeled *A*, *B*, *C*) are observed for the saturated solution of L-proline, $\chi_{pro} = 0.20$. As the mole fraction of L-proline decreases, the peak intensities of *A* and *C* decrease, leaving peak *B* as the only distinguishable peak at the lowest mole fraction, $\chi_{pro} = 0.05$ (approximately 2.2 mol L^{-1}). In Fig. 2b, the mole fraction of L-proline is held constant at $\chi_{pro} = 0.20$ while w varies from 1.1 to 12. Four distinct solute peaks (labeled *A*, *B*, *C*, *D*) are visible in all spectra. As expected, the peaks become more prominent as the overall amount of L-proline in the sample increases from $w = 1.1$ to $w = 5$. However, this trend does not continue for $w > 7$ where a significant portion of the spectrum exhibits negative optical density changes (see below). In Fig. 2c, the

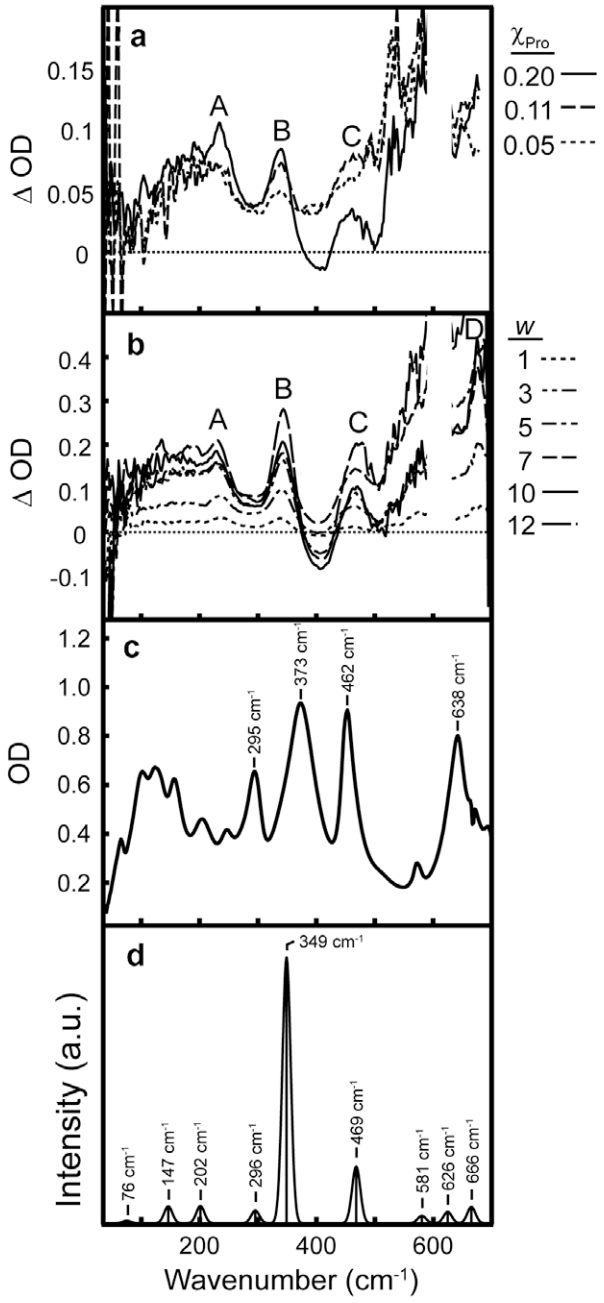

Fig. 2. Terahertz absorption spectra of aqueous L-proline in 0.024 mol L^{-1} AOT/heptane reverse micelles. Difference spectra of L-proline only (water contribution subtracted; see text) are shown in (a) and (b). Pathlength is 4.2 mm in (a) and 1.9 mm in (b). (c) Absorption spectrum of solid L-proline and (d) calculated DFT spectrum of gas-phase L-proline.

solid-phase absorption spectrum of L-proline is shown for comparison. Four distinct, narrow absorption peaks are observed at 295, 373, 462, and 638 cm^{-1}. Based on their similar frequencies and intensities, we suggest that the modes responsible for these peaks in the solid phase are the same modes observed in the difference spectra of aqueous L-proline.

Clues to the nature of these modes can be found upon closer examination of Fig. 2. The absorption peaks in Fig. 2a exhibit no frequency shift as the mole fraction of L-proline in water increases. However, two of the peaks in Fig. 2b shift as *w* increases. These results are summarized in Table 1. Both peaks *A* and *C* show significant shifts in frequency. Peak *A* experiences an overall 8 cm^{-1} red shift as *w* increases from 1 to 12 and peak *C* experiences a 16-cm^{-1} blue shift for the same *w* values; however, peaks *B* and *D* do not shift. Since an increase in *w* correlates with an increase in size for L-proline-containing reverse micelles (see below), this suggests that the modes responsible for peaks *A* and *C* are sensitive to the size of the reverse micelle. Additionally, we dissolved L-proline in D_2O in order to deuterate the labile amine and carboxylic acid hydroxyl protons. This solution was encapsulated in AOT reverse micelles resulting in the difference spectrum shown in Fig. 3. Comparison of this difference spectrum with the equivalent solution of reverse micelles containing L-proline in H_2O reveals that both peaks *B* and *D* experience significant red shifts of 11 cm^{-1} and 9 cm^{-1} while peaks *A* and *C* are nearly unperturbed. Thus, we can assign the modes responsible for peaks *B* and *D* to significant motion of the amine or hydroxyl protons in L-proline. The measured frequency shifts are listed in Table 2.

Table 1
Terahertz frequency peak shifts of aqueous L-proline (χ_{pro} = 0.2) in reverse micelles as a function of *w*.

w	*A* (cm^{-1})	*B* (cm^{-1})	*C* (cm^{-1})	*D* (cm^{-1})
1	237	339	453	680
3	235	340	462	679
5	230	342	467	681
7	229	341	466	679
10	229	342	466	682
12	228	343	469	–[b]
Δ[a]	−8	+3	+16	+2

[a] Δ represents the total shift in center frequency as *w* changes from 1 to 12. A negative shift indicates a red shift and a positive shift indicates a blue shift. The total increase in hydrodynamic radius represented by these *w* values is ~2 nm. Estimated error in Δ = ±1 cm^{-1}.
[b] The peak location could not be determined due to noise in the difference spectrum.

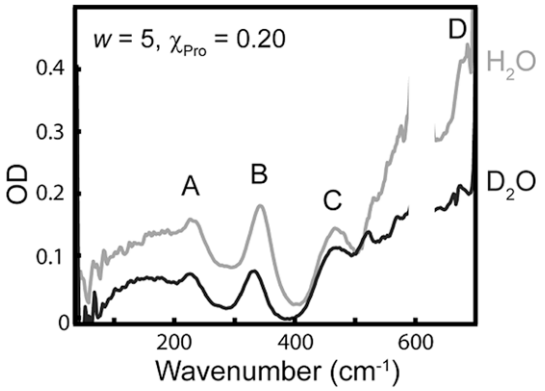

Fig. 3. Comparison of the terahertz absorption spectra of aqueous L-proline dissolved in H_2O and D_2O and encapsulated within 0.024 mol L^{-1} AOT/heptane reverse micelles.

Table 2
Frequency peak shifts of aqueous L-proline (χ_{pro} = 0.2) in reverse micelles (*w* = 5) dissolved in H_2O and D_2O.

Solvent	*A* (cm^{-1})	*B* (cm^{-1})	*C* (cm^{-1})	*D* (cm^{-1})
H_2O	230	342	467	681
D_2O	225	331	466	672
Δ[a]	−5	−11	−1	−9

[a] Δ represents the shift in center frequency as the solvent changes from H_2O to D_2O. A negative shift indicates a red shift and a positive shift indicates a blue shift. Estimated error in Δ = ±1 cm^{-1}.

To further illuminate our understanding of low-frequency modes of L-proline, we performed GAUSSIAN-03 calculations to model the unsolvated vibrational spectrum of L-proline and visualize its mode behavior [9,23]. We used the zwitterionic solid-state X-ray structure of the protonated [24] and corresponding deuterated species, and performed B3LYP/DFT frequency and intensity calculations using the 6-311+g(d) basis set with structure optimization. Selecting higher-level electron bases did not change the calculated frequencies but significantly extended calculation times. To mimic the experimental spectrum, bandwidths were generated by convolving the GAUSSIAN-03 intensity output with a Gaussian function having a full width half maximum of 25 cm^{-1}. While a solid-state periodic boundary DFT calculation would be more appropriate to extract lowest frequency intermolecular vibronic modes [1], the results from the GAUSSIAN-03 calculation, which only identifies intramolecular modes, agrees reasonably well with the solid-state and aqueous-phase terahertz spectra (see Fig. 2d). Four strongly absorbing modes are identified in the region between 200 cm^{-1} and 600 cm^{-1} with positions and relative intensities similar to the experimental results. These modes originate from motion of all atoms; however, the collective motions responsible for peak *B* are dominated by large amplitude motion of the zwitterionic amine-hydrogen atom shared between the nitrogen and the nearest carboxyl oxygen. Because of its potential for strong interaction with solvent, relatively minor structural changes, and susceptibility to deuteration, we expect frequency shifts and intensity changes of mode *B* to be most sensitive to aqueous solvation. These expectations agree with the calculated vibrational spectrum for deuterated L-proline species (not shown), as well as the experimental solvation and isotopic substitution observations discussed above. Further modeling with hydrogen-bonded solvent or water-bridges is clearly warranted to gain a better picture of the experimental observations.

In addition to the relatively narrow solute peaks observed in Fig. 2a and b, we also observe two broad absorption features. One is centered at ~150 cm^{-1} while another weak band occurs for frequencies >400 cm^{-1}. Bands with frequencies <300 cm^{-1} are typically assigned to intermolecular, hydrogen-bonding modes. For the L-proline aqueous solution, the 150 cm^{-1} feature could be the result of hydrogen bonding between L-proline and water, neighboring L-proline molecules (for $\chi_{pro} = 0.20$, each L-proline molecule is solvated by approximately 4 water molecules), or both. The group of bands in the solid-phase spectrum centered at ~120 cm^{-1} most likely originates from solid phonon bands, which are due to intermolecular hydrogen bonding within the solid matrix. Assignment of the 400 cm^{-1} absorption feature is more difficult. It is tempting to suggest that this feature is due to a subtraction error since this feature occurs in the same spectral region as the librational mode of water in AOT reverse micelles. This subtraction error might also explain the broad absorption near 150 cm^{-1}. However, both of these broad absorption features are also visible in the difference spectrum when L-proline is dissolved in D_2O (Fig. 3), despite the fact that the librational band of D_2O in AOT reverse micelles is red-shifted by >100 cm^{-1}.

As noted above, several difference spectra of L-proline within reverse micelles in Fig. 2b exhibit significant regions of negative optical density change. If our assumption that the intensity contributions from L-proline and water are independent and additive, then one would expect only positive optical density changes after ratioing L-proline spectra against water-only spectra for the same *w* value. One complication to performing the subtraction, which generates the difference spectra, is the choice of water spectra. We naively performed the subtraction for solutions with the same water-to-surfactant mole ratio, *w*, assuming that L-proline-filled reverse micelles and water-filled reverse micelles of equivalent *w* have the same number and 'type' of water molecules within both reverse micelle systems. However, Fig. 1a reveals that the absorption of H_2O within AOT reverse micelles is most sensitive to *w*, and therefore the size of the reverse micelles, in the spectral region between 350 cm^{-1} and 550 cm^{-1}. This is identical to the region in which negative optical density changes are observed for L-proline encapsulated within AOT reverse micelles.

Because the concentration of the L-proline solution is significant in these cases, L-proline-filled and water-filled reverse micelles of equivalent *w* are likely to be significantly different in size, causing the water to experience different interactions or degrees of confinement. Thus, it may be inappropriate to subtract the absorption spectrum of equivalent *w*, and could result in 'over-subtraction' between 350 cm^{-1} and 550 cm^{-1}. To explore this issue further, dynamic light scattering measurements were performed to obtain the hydrodynamic radius of the reverse micelles containing L-proline (see Fig. 4). Each sample was measured at 25 °C and two detection angles, 30° and 90°, using a Scitech, Inc. ST-100 Variable Angle Light Scattering Instrument. The hydrodynamic radius was determined by a standard fitting procedure [9,25]. Measurements for reverse micelles containing L-proline were compared to measurements obtained for water-only filled reverse micelles of the same *w* value. These data indicate that radii for both *w* values of L-proline-filled reverse micelles examined are significantly (~1.5 times) larger than the radii of the corresponding water-filled reverse micelles. Consequently, the $w = 10$, L-proline-filled reverse micelle is more similar in size to a $w = 20$ or $w = 25$, water-filled reverse micelle. Therefore, we attempted to subtract both of these water spectra from the $w = 10$ L-proline-water absorption spectrum, but the negative optical density change remained in both cases. One way to eliminate the possibility of a subtraction error due to size discrepancies is to encapsulate L-proline within Brij-30 reverse micelles. The absorption spectra of water in Brij-30 reverse micelles, shown in Fig. 1c and d, have minimal dependence on *w* and reverse micelle size. Unfortunately, all attempts to prepare stable Brij-30 reverse micelles containing concentrated L-proline failed. It is also possible that the negative intensities observed in the difference spectra are due to highly correlated absorptive properties of water and L-proline [26] or water exclusion effects. In addition, at these high-L-proline concentrations, the spectra may be influenced by strongly associated water of hydration (water-bridges), L-proline self-association to form multimers, or surfactant interfacial charge effects. Further investigations are underway to understand the origin of these unusual spectral observations of L-proline within AOT reverse micelles.

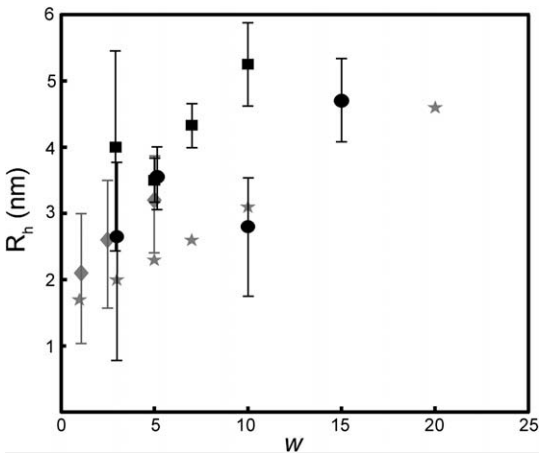

Fig. 4. Hydrodynamic radii of 0.10 mol L^{-1} AOT/heptane reverse micelles filled with aqueous L-proline, $\chi_{pro} = 0.2$, are shown as a function of *w* (squares) with estimated error limits. For comparison, hydrodynamic radii of H_2O-filled reverse micelles are also presented: 0.10 mol L^{-1} AOT/heptane (circles), 0.10 mol L^{-1} AOT/cyclohexane (stars) [10], and 0.20 mol L^{-1} Brij-30/cyclohexane (diamonds) [12].

4. Conclusions

An approach for obtaining terahertz spectra of aqueous biomolecular species in reverse micelles is presented, and details concerning the observed water spectra, such as the effect of reverse micelle size and choice of surfactant, are discussed. The amino acid, L-proline, was encapsulated within AOT surfactant and dispersed in *n*-heptane. Spectra of L-proline, solvated by both H_2O and D_2O, were obtained at room temperature as a function of L-proline concentration in various-sized reverse micelles, and four low-frequency modes (<700 cm^{-1}) were observed for aqueous concentrations greater than 3 mol L^{-1}. These features correlate with absorptions observed in solid-phase L-proline and modeled by GAUSSIAN-03 DFT calculations. In addition, the modes are found to shift in frequency, by approximately 10 cm^{-1}, with changes in reverse micelle size and amine-hydrogen deuteration. Anomalous 'negative' absorption in the spectral region of 350 cm^{-1}–650 cm^{-1} occurs for concentrations of L-proline near saturation, suggesting the presence of strong intermolecular interactions, surface charge, or water exclusion effects. In addition, qualitative differences in the water spectra are observed when comparing H_2O and D_2O encapsulated within AOT and Brij-30 reverse micelles. The new observations presented in this Letter require further investigation, and related studies of other biomolecular species will be reported in future publications.

Acknowledgements

We are grateful to Dr. Jeffrey Owrutsky from the US Naval Research Laboratory for helpful insights, motivation, and discussions in preparing reverse micelle samples used in this work. Special thanks to Dr. Li-Piin Sung of the NIST Building and Fire Research Laboratory for allowing us to use her Dynamic Light Scattering apparatus and helping us perform data analysis. B.G. gratefully acknowledges support from the National Science Foundation under Agreement No. PHY-0453430. Any opinions, findings, and conclusions or recommendations expressed are those of the author(s) and do not necessarily reflect the views of the National Science Foundation.

References

[1] D.F. Plusquellic, K. Siegrist, E.J. Heilweil, O. Esenturk, Chem. Phys. Chem. 8 (2007) 2412.
[2] A.G. Markelz, J.R. Knab, J.Y. Chen, Y. He, Chem. Phys. Lett. 442 (2007) 413.
[3] J.D. Eaves, C.J. Fecko, A.L. Stevens, P. Peng, A. Tokmakoff, Chem. Phys. Lett. 376 (2003) 20.
[4] G. Giraud, K. Wynne, J. Am. Chem. Soc. 124 (2002) 12110.
[5] N.T. Hunt, L. Kattner, R.P. Shanks, K. Wynne, J. Am. Chem. Soc. 129 (2007) 3168.
[6] J.E. Bertie, Z. Lan, Appl. Spectrosc. 50 (1996) 1047.
[7] T.C. Wong, in: P. Somasundaran, A. Hubbard (Eds.), Encyclopedia of Surface and Colloid Science, Taylor and Francis, London, 2006.
[8] A.J. Wand, M.R. Ehrhardt, P.F. Flynn, Proc. Natl. Acad. Sci. 95 (1998) 15299.
[9] Certain commercial equipment, instruments, or materials are identified in this Letter to adequately specify the experimental procedure. In no case does identification imply recommendation or endorsement by NIST, nor does it imply that the materials or equipment identified are necessarily the best available for the purpose.
[10] A. Maitra, J. Phys. Chem. 88 (1984) 5122.
[11] M. Zulauf, H.F. Eicke, J. Phys. Chem. 83 (1979) 480.
[12] D. Pant, N.E. Levinger, Langmuir 16 (2000) 10123.
[13] D.S. Venables, K. Huang, C.A. Schmuttenmaer, J. Phys. Chem. B 105 (2001) 9132.
[14] Q. Zhong, D.A. Steinhurst, E.E. Carpenter, J.C. Owrutsky, Langmuir 18 (2002) 7401.
[15] D. Mittleman, M.C. Nuss, V. Colvin, Chem. Phys. Lett. 275 (1997) 332.
[16] J.E. Boyd, A. Briskman, C.M. Sayers, D. Mittleman, V. Colvin, J. Phys. Chem. B 106 (2002) 6346.
[17] H. MacDonald, B. Bedwell, G. Erdogan, Langmuir 2 (1986) 704.
[18] G. Onori, A. Santucci, J. Phys. Chem. 97 (1993) 5430.
[19] I.R. Piletic, D.E. Moilanen, D.B. Spry, N.E. Levinger, M.D. Fayer, J. Phys. Chem. A 110 (2006) 4985.
[20] D.E. Moilanen, N.E. Levinger, D.B. Spry, M.D. Fayer, J. Am. Chem. Soc. 126 (2007) 14311.
[21] G.E. Walrafen, Water: A Comprehensive Treatise, Plenum, New York, 1972.
[22] D.E. Rosenfeld, C.A. Schmuttenmaer, J. Phys. Chem. B 110 (2006) 14304.
[23] J.A. Pople et al., GAUSSIAN 03, Revision B.04, Gaussian, Inc., Pittsburgh, PA, 2003.
[24] R.L. Kayushin, B.K. Vainshte, Soviet Phys. Crystallogr. 10 (1966) 698.
[25] R. Pecora, Dynamic Light Scattering: Applications of Photon Correlation Spectroscopy, Plenum Press, New York, 1985.
[26] U. Heugen, G. Schwaab, E. Bruendermann, M. Heyden, X. Yu, D.M. Leitner, M. Havenith, Proc. Natl. Acad. Sci. 103 (2006) 12301.
[27] H.R. Zelsmann, J. Mol. Struct. 350 (1995) 95.